Hepatocyte Polarization Is Essential for the Productive Entry of the Hepatitis B Virus

Andreas Schulze,[1]* Kerry Mills,[2]* Thomas S. Weiss,[3] and Stephan Urban[1]

Human hepatitis B virus (HBV) is characterized by a high species specificity and a distinct liver tropism. Within the liver, HBV replication occurs in differentiated and polarized hepatocytes. Accordingly, the *in vitro* HBV infection of primary human hepatocytes (PHHs) and the human hepatoma cell line, HepaRG, is restricted to differentiated, hepatocyte-like cells. Though preparations of PHH contain up to 100% hepatic cells, cultures of differentiated HepaRG cells are a mixture of hepatocyte-like and biliary-like epithelial cells. We used PHH and HepaRG cells and compared the influence of virus inoculation dose, cell differentiation, and polarization on productive HBV infection. At multiplicities of genome equivalents (mge) >8,000, almost 100% of PHHs could be infected. In contrast, only a subset of HepaRG cells stained positive for HBcAg at comparable or even higher mge. Infection predominantly occurred at the edges of islands of hepatocyte-like HepaRG cells. This indicates a limited accessibility of the HBV receptor, possibly as a result of its polar sorting. Multidrug resistance protein 2 (MRP2), a marker selectively transported to the apical (i.e., canalicular) cell membrane, revealed two polarization phenotypes of HepaRG cells. HBV infection within the islands of hepatocyte-like HepaRG cells preferentially occurred in cells that resemble PHH, exhibiting canalicular structures. However, disruption of cell-cell junctions allowed the additional infection of cells that do not display a PHH-like polarization. *Conclusion:* HBV enters hepatocytes via the basolateral membrane. This model, at least partially, explains the difference of PHH and HepaRG cells in infection efficacy, provides insights into natural HBV infection, and establishes a basis for optimization of the HepaRG infection system. (HEPATOLOGY 2012;55:373-383)

Human hepatitis B virus (HBV), a small, enveloped DNA virus, is the prototypic member of the family, *hepadnaviridae*, causing acute and persistant liver infections.[1] Currently, 360 million people are chronically infected with HBV and are, consequently, prone to developing progressive liver diseases, such as cirrhosis or hepatocellular carcinoma. Hepadnaviruses exhibit a pronounced liver tropism and a narrow host range.[2] HBV predominantly infects and replicates in hepatocytes, but virus-specific antigens and nucleic acids have also been found in a number of nonhepatic tissues, including kidney, pancreas, and peripheral blood mononuclear cells.[3] However, whether replication in extrahepatic tissues contributes to virus propagation is unclear.[4,5] The preference for replication in the liver can only partially be explained by hepatocyte-specific transcription factors.[6] Further liver specificity occurs at the stage of early infection, because the differentiation state of HepaRG cells and primary hepatocytes is a prerequisite for the expression of an HBVpreS1-specific receptor and subsequent infection (Meier et al., manuscript in preparation).

Abbreviations: cccDNA, covalently closed circular DNA; DMSO, dimethyl sulfoxide; EGTA, ethylene glycol tetraacetic acid; ELISA, enzyme-linked immunosorbent assay; HBcAg, hepatitis B core antigen; HBsAg, hepatitis B surface antigen; HBV, hepatitis B virus; IF, immunofluorescence; mge, multiplicity of genome equivalents; mRNA, messenger RNA; MRP2, multidrug resistance protein 2; PBS, phosphate-buffered saline; PHHs, primary human hepatocytes; p.i., postinfection; S/N, signal-to-noise ratio.

From the [1]Department of Infectious Diseases, Molecular Virology, Otto-Meyerhof-Zentrum, University Hospital Heidelberg, Heidelberg, Germany; [2]Food Standards Australia New Zealand, Canberra, Australia; and [3]Department of Pediatrics and Adolescent Medicine, University Hospital Regensburg, Regensburg, Germany.

Received April 18, 2011; accepted September 19, 2011.

This work was supported by the Deutsche Forschungsgemeinschaft (grant numbers UR 72/4-3 and UR 72/5-1 FOR-1202 "Mechanisms of persistence of hepatotropic viruses"). K.M. was supported by a World Health Organization International Agency for Research on Cancer fellowship and a European Commission Marie Curie Incoming International Fellowship.

**These authors contributed equally to the work.*

Address reprint requests to: Stephan Urban, Ph.D., Department of Infectious Diseases, Molecular Virology, Otto-Meyerhof Zentrum, University Hospital Heidelberg, Im Neuenheimer Feld 350, 69120 Heidelberg, Germany. E-mail: Stephan.Urban@med.uni-heidelberg.de; fax: +49-6221-56-1946.

View this article online at wileyonlinelibrary.com.

DOI 10.1002/hep.24707

Potential conflict of interest: Nothing to report.

Additional Supporting Information may be found in the online version of this article.

Two strategies are used for the investigation of HBV infection *in vitro*. One is the application of hepatoma cell lines (e.g., HuH7 or HepG2), which do not support HBV entry and hence cannot be infected, but allow viral replication after delivery of the viral genome by stable or transient transfection.[7,8] These cell lines allow the examination of late-replication steps, such as transcription, translation, assembly, and release of HBV particles. Alternatively, primary cultures of human[9] or tupaia[10] hepatocytes and the human hepatoma cell line, HepaRG,[11] support HBV infection and replication and are employed for investigations addressing HBV entry (e.g., attachment, receptor interaction, viral uptake, covalently closed circular DNA [cccDNA] formation, and regulation of gene transcription). Important determinants for infectivity within the HBV envelope proteins were identified using mutational analyses. These include the N-terminal 75 amino acids of the preS1-domain of the HBV L-protein, its myristoylation, and the integrity of a region in the antigenic loop of the S-domain.[12-15] Little is known about specific host factors, particularly HBV-specific receptor(s) that contribute to the tropism of the virus. We and others identified heparan sulfate proteoglycans as mandatory attachment factors for HBV.[16,17] However, because of their ubiquitous expression, this interaction does not explain the hepatotropism of HBV, but rather represents a first, nonspecific step of a multistep entry process. Potential HBV-receptor candidates have been described in the past, but none of them have been confirmed in a functional assay.[2] Expression and accessibility of HBV-specific receptor(s) on the cell surface define, among other factors, the susceptibility of cells toward HBV. In contrast to most epithelial cells, which exhibit a polarity consisting of a single apical and basal pole that oppose each other, hepatocytes in the liver are polarized in a more complex manner, with distinct apical and basolateral domains facing the continuous network of bile canaliculi and the hepatic sinusoid.[18] Tight junctions between hepatocytes prevent lateral diffusion of substrates, form the blood-bile barrier, and contribute to the maintenance of cell polarity.

Using HepaRG cells and primary human hepatocytes (PHHs), we performed a detailed analysis of the properties of *in vitro* HBV infection. We investigated whether cell polarization, in addition to cell differentiation, would play a role in the infection process. We took advantage of the fact that HepaRG cells, in contrast to other hepatoma-derived cell lines, constitutively and synchronously display both hepatocyte- and biliary-like epithelial phenotypes at confluence.[19]

We demonstrated that disrupting the epithelial barrier leads to an increased HBV infection, suggesting that the entry of HBV into hepatocytes occurs in a polarized manner and that hepatocyte polarization imposes a physical barrier that restricts the access of the virus to its receptor(s).

Materials and Methods

Cell Lines. HepaRG cells were cultivated as previously described.[11] Tissue samples from liver resections were obtained from patients undergoing partial hepatectomy. Experimental procedures were performed according to Human Tissue and Cell Research Foundation guidelines, with informed patient consent approved by the Ethical Committee of the University of Regensburg (Regensburg, Germany). PHHs were isolated, as previously described,[20] and seeded at 1.7×10^5 cells/cm^2 in HepaRG maintenance medium supplemented with 2 mM of L-glutamine. They were refreshed with the same medium, supplemented with 0.5% dimethyl sulfoxide (DMSO), 4 hours and 1 day postplating.

HBV Infection Assays. As infectious inocula, 100-fold concentrated supernatants of HepAD38 or HepG2.2.15 cells, were used. Differentiated HepaRG cells or PHHs were incubated with dilutions of the virus stock in medium supplemented with 4% polyethylene glycol 8000 for 20-24 hours at 37°C. Cells were washed extensively and further cultivated with regular medium exchange. Secreted hepatitis B surface antigen (HBsAg) was determined qualitatively (AxSYM, signal-to-noise ratio [S/N]; Abbott, Wiesbaden-Delkenheim, Germany) or quantitatively (ARCHITECT, IU/mL; Abbott). All infection experiments were performed in duplicate and repeated at least twice with different cell passages.

Ethylene Glycol Tetraacetic Acid–Induced Disruption of Tight Junctions. HepaRG cells were preincubated for 30 minutes at 37°C with 800 μM of ethylene glycol tetraacetic acid (EGTA) in HepaRG differentiation medium or Ca^{2+}-free buffer. Following preincubation, cells were washed with phosphate-buffered saline (PBS) and inoculated with HBV either in the presence or absence of EGTA in differentiation medium for 20-24 hours at 37°C.

Immunofluorescence Analyses. Cells were fixed with 4% paraformaldehyde, permeabilized with 0.25% Triton-X-100, and incubated overnight at 4°C with a hepatitis B core antigen (HBcAg)-specific polyclonal antibody (H363) at 1:1,000 (a gift from Heinz Schaller, ZMBH, University of Heidelberg, Germany) (Heinz Schaller, the Center for Molecular Biology at

the University of Heidelberg, Heidelberg, Germany), a HBsAg-specific monoclonal antibody (NCL) at 1:100 (Novocastra Laboratories Ltd., Newcastle upon Tyne, UK), a multidrug-resistant protein 2 (MRP2)-specific polyclonal antibody (EAG5) at 1:100 (Dietrich Keppler, Deutsches Krebsforschungszentrum, Heidelberg, Germany), and/or an MRP2-specific monoclonal antibody (IQP-178P, clone M2 III-6) at 1:30 (IQ Products, Groningen, The Netherlands). Cells were washed and incubated in the dark for 1 hour at room temperature with a 1:250 or 1:500 dilution of an Alexa 488– or Alexa 546–conjugated secondary antibody (Invitrogen, Karlsruhe, Germany). Nuclei staining was performed either during secondary antibody incubation with bisBenzimid-H(oechst)33342-trihydrochlorid (1 μg/mL) or, subsequently, for 30 minutes with 4′,6′-diamidino-2′-phenylindole dihydrochloride (1 μg/mL). Images were acquired with an inverted fluorescence microscope (Leica, Wetzlar, Germany). All images were made under comparable settings and, after, handled identically. Images were analyzed using ImageJ software. The nucleus-counter function of the WCIF plug-in was used to count the number of labeled nuclei. The cell-counter plug-in was used to count the number of HBcAg-positive cells.

Results

Comparative Infection of PHH and HepaRG Cells With HBV. HepaRG cells acquire susceptibility toward HBV infection only after a preceding treatment with DMSO. This has been attributed to a DMSO-induced differentiation of the bipotent HepaRG progenitor cells into hepatic and biliary-like cells.[19] To analyze critical parameters that influence and, possibly, restrict the susceptibility of HepaRG cells and PHHs, we compared HBV infection using both systems. In a first experiment, we infected freshly prepared PHH with a multiplicity of HBV genome equivalents (mge) of 8×10^4 and analyzed HBsAg expression by immunofluorescence (IF) at day 12 postinfection (p.i.). Approximately 99% of PHHs stained positive for HBsAg at this high inoculation dose (Fig. 1A, first row). Nevertheless, infection could be blocked by using the previously characterized HBVpreS1-lipopeptide HBVpreS/2-48^{myr},[21] excluding unspecific entry (Fig. 1A, second row). To investigate the dependency of HBV-infection efficacy on the inoculation dose, we applied increasing mge and quantified the percentage of HBcAg-positive cells and the secreted HBsAg (Fig. 1B, top). After inoculation of the cells for 20 hours with an mge of 0.8×10^4, 98% of PHHs became

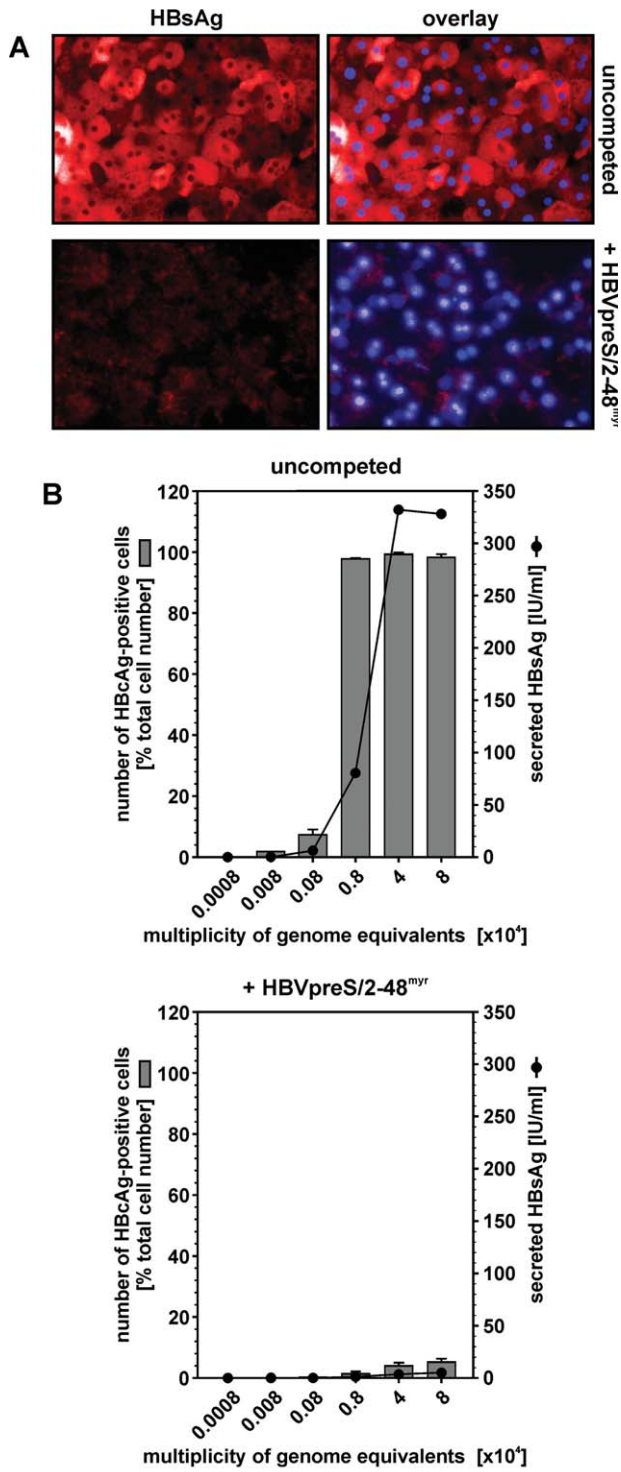

Fig. 1. Analysis of HBV infection of PHHs. (A) HBsAg-specific IF (red) and overlay images with the nuclei stain (blue) of HBV infections (8×10^4 ge/cell) of PHHs (day 12 p.i., 400× magnification). First row: uncompeted infection. Second row: infection after preincubation for 30 minutes at 37°C with 100 nM of HBVpreS/2-48^{myr}. (B) PHHs were infected with 0.0008, 0.008, 0.08, 0.8, 4, or 8×10^4 HBV ge/cell. In parallel, PHHs were incubated for 30 minutes at 37°C with 100 nM of HBVpreS/2-48^{myr} and infected with HBV in the presence of the inhibitor. Secreted HBsAg from day 4-7 p.i. was quantified by enzyme-linked immunosorbent assay (ELISA) (circles). The number of HBcAg-positive cells was determined by IF on day 7 p.i. and presented as a percentage of the total cell number (n = 12,099) (bars).

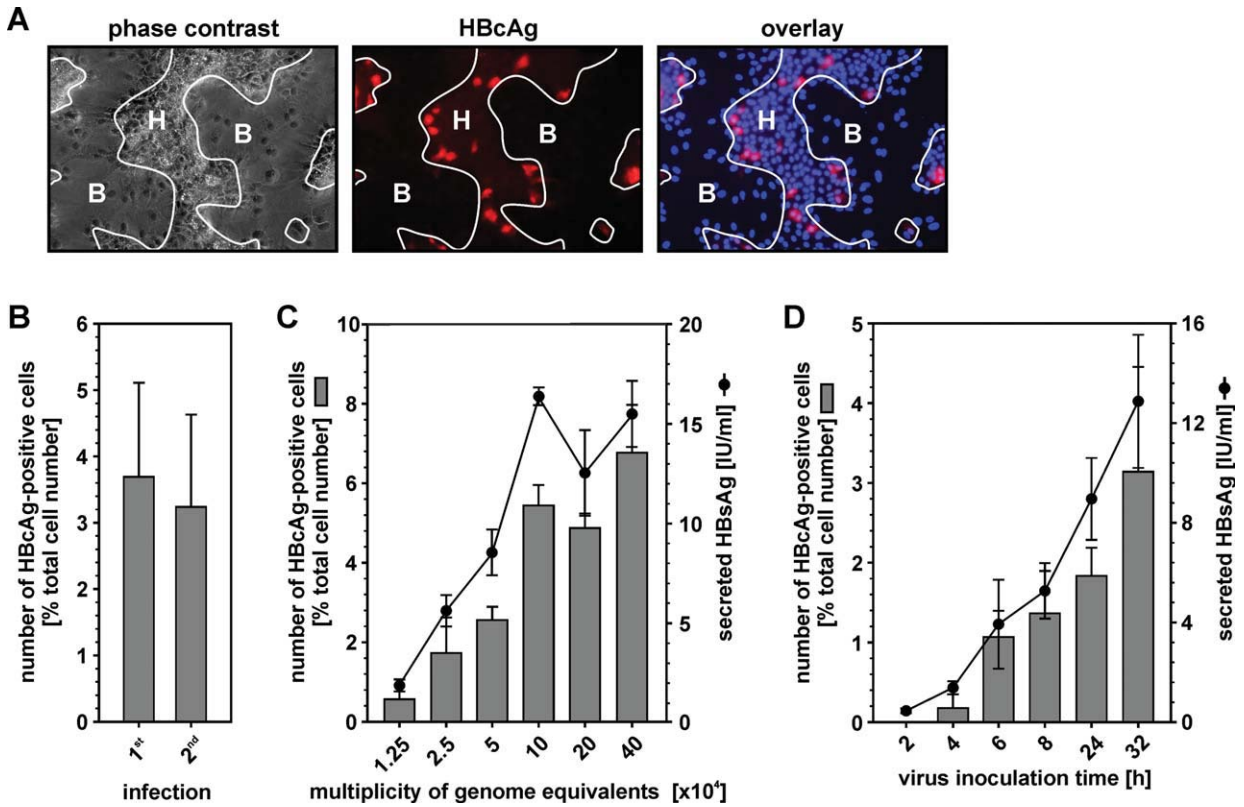

Fig. 2. Analysis of HBV infection of HepaRG cells. (A) Cells were infected with 4×10^4 HBV ge/cell. Shown are a phase-contrast image, an HBcAg-specific IF (red), and an overlay of the IF with a nuclei stain in blue (day 12 p.i., 200× magnification; H = hepatocyte-like cells; B = biliary-like cells). (B) HepaRG cells were infected with 4×10^4 HBV ge/cell. After 20 hours of inoculation, the virus-containing supernatant was removed and used to infect new HepaRG cells. At day 12 p.i., cells of the first and second round of infection were analyzed by HBcAg-specific IF. The number of HBcAg-positive cells is presented as a percentage of the total cell number counted (n = 45,186). (C) HepaRG cells were infected with 1.25, 2.5, 5, 10, 20, or 40×10^4 HBV ge/cell. Secreted HBsAg from days 7-11 p.i. was quantified by ELISA (circles). On day 11 p.i., cells were analyzed by IF for HBcAg-positive cells (bars). Results are presented as a percentage of the total cell number (n = 27,457). (D) HepaRG cells were inoculated with 4×10^4 HBV ge/cell for 2, 4, 6, 8, 24, or 32 hours. On day 11 p.i., the secreted HBsAg was measured by ELISA (circles). In parallel, an HBcAg-specific IF was performed. The number of HBcAg-positive cells (bars) is presented as the percentage of the total cell number (n = 37,121).

infected. An increase of mge from 0.8×10^4 to 4×10^4 resulted in a 4.1-fold change of secreted HBsAg, despite saturation in the number of infected cells. This indicates multiple infection events per cell. However, raising the mge to 8×10^4 ge/cell did not lead to a further increase of HBsAg secretion, indicating that either the number of cccDNA templates within cells remained constant, despite more incoming relaxed circular DNA copies, or that transcription from cccDNA is regulated. To rule out that the HBsAg measured in the cell-culture supernatant was caused by unspecific and receptor-independent delivery of HBV genomes at this very high mge, we inhibited infection using 100 nM of HBVpreS/2-48^{myr} (Fig. 1B, bottom). At an mge of 0.8×10^4, infection could be reduced from 98% to 1.3% of cells. Even at higher virus concentrations, the peptide was still inhibiting more than 95% of infection.

Similarly to PHHs, differentiated HepaRG cells were infected with an mge of 4×10^4 and analyzed by IF for HBcAg expression at day 12 p.i. (Fig. 2A). In contrast to PHHs, only a subset of HepaRG cells (7%) expressed HBcAg. This subset of infected cells locates within islands of hepatic cells, which are characterized by dense accumulation of smaller nuclei with a roundish shape (marked with H). No HBcAg-specific staining was observed in the biliary-like cells (marked with B), indicating that they are refractory to infection. The fraction of hepatocyte-like cells significantly varies between different HepaRG cell batches and passages (45%-90%; data not shown). Infected cells within hepatic islands are predominantly located at the edges (Fig. 2A). To investigate whether the observed low infection rate is caused by inefficient binding or uptake of virions, we transferred the virus-containing supernatant of a first round of infection to

new HepaRG cells (Fig. 2B). An only slightly reduced number of HBcAg-positive cells was observed (3.7%-3.2%). This indicates that virions are still present in the inoculum even after 20 hours of inoculation with HepaRG cells, arguing for a slow, inefficient adsorption of virus to the target cell. To investigate whether this restriction could be overcome by higher inoculation doses, we increased the mge and quantified the number of HBcAg-positive cells and secreted HBsAg (Fig. 2C). Only 0.6% of HepaRG cells were infected at an mge of 1.25×10^4. Increase of the inoculum to 10×10^4 ge/cell resulted in the increase of secreted viral markers and in a higher percentage of infected cells (5.4%). A further increase of the mge to 40×10^4 did not result in higher infection rates. Thus, hepatic cells are principally susceptible, but subjected to a restriction, when compared with PHHs.

To analyze whether HBV infection depends on inoculation time, we infected HepaRG cells for 2-32 hours and determined the number of HBcAg-positive cells and HBsAg secretion (Fig. 2D). Longer inoculation times led to a linear increase in the number of HBcAg-positive cells and the amount of secreted HBsAg. However, a maximum of 3.1% of all cells were infected after 32 hours of inoculation. These results demonstrate an initial, time, and virus-titer–dependent, diffusion-controlled process of HBV infection that, in the case of HepaRG cells, only leads to limited productive infection.

Characterization of the Polarization of PHH and HepaRG Cells and Its Role for HBV Infection. PHHs were infected with HBV and stained for HBsAg and the MRP2 as a polarization marker on day 12 p.i. (Fig. 3A). In hepatocytes, MRP2 is exclusively sorted to the apical (canalicular) membrane.[22] PHH uniformly displayed a hepatocyte-like phenotype with canalicular structures. Almost 100% of the infected PHHs stained HBsAg positive. It has been described that the hepatocyte-like HepaRG cells exhibit a phenotype close to that of human hepatocytes with functional, canaliculus-like structures.[19] To analyze the expression of MRP2 in HepaRG cells before and during DMSO-induced differentiation, we performed MRP2-specific IF at 10 time points throughout the 4-week cultivation process (Fig. 3B; Supporting Fig. 1). A maximum of 0.15% of the cells showed a canalicular MRP2-localization within the first 2 weeks after seeding. Two days after the first addition of DMSO on day 14 postseeding, 6% of cells were positive for a canalicular MRP2 signal. This fraction increased to 26% at day 29 postseeding. This demonstrates a direct link between the induction of differentiation and polarization in HepaRG cells. In contrast to PHH, differentiated HepaRG cells revealed different patterns of MRP2 expression (Fig. 3C; Supporting Fig. 2). Though MRP2 was not detectable in biliary-like cells, hepatocyte-like cells showed two different patterns of MRP2 distribution. One subset displayed a PHH-like canalicular MRP2 localization between two or more differentiated cells. The other subset showed a dispersed MRP2 signal. The ratio between canalicular and disperse MRP2 signals differed considerably between HepaRG cell batches and passages, indicating variable degrees of canalicular organization of the apical membrane (Supporting Fig. 2). To analyze possible consequences for HBV-infection efficacy, two batches of HepaRG cells, designated A and B, were cultivated under identical conditions. Cell batch A showed a comparable ratio of hepatic to biliary-like cells (47%-53%), whereas in cell batch B, 6 times more hepatocyte-like cells than biliary-like cells were observed (85%-15%) (data not shown). Cell batch B, which had a 1.8-fold higher number of hepatocyte-like cells, compared to batch A, showed an 8-fold increased number of hepatic cells with canalicular MRP2 signals (Fig. 3D, black bars). Accordingly, HBV infection revealed a 7.5 times higher infection rate in cell batch B (Fig. 3D, gray bars). This increase cannot be explained by a higher degree of differentiation, but is more likely to be the result of an elevated number of hepatocyte-like cells containing a canalicular MRP2 signal. We, therefore, hypothesize that PHH-like polarized HepaRG cells containing canalicular structures allow better access to the HBV receptor(s) where non-PHH-like differentiated HepaRG cells do not.

Cell-Cell Junctions as Physical Barriers for the Access of HBV to Specific Receptor(s) in Noncanalicular Hepatic HepaRG Cells. The aforementioned restriction of infection in differentiated HepaRG cells raised the question of which factor(s) might be responsible. Because we found a preferential infection of HepaRG cells on or close to the outer rim of hepatic islands (Fig. 2A) and an increased infection rate in HepaRG cells forming canaliculi (Fig. 3D), we hypothesized a physical obstruction resulting from the induced differentiation and polarization process. If HBV infection proceeds through entry via the basolateral membrane, a physical barrier might be caused by tight junctions preventing access to basolateral localized receptor(s). We, therefore, treated differentiated HepaRG cells 30 minutes before infection with EGTA to complex Ca^{2+} ions and destabilize the tight junctions. Preincubation of HepaRG cells with 800 μM of EGTA resulted in 2.4-fold increased HBsAg, as

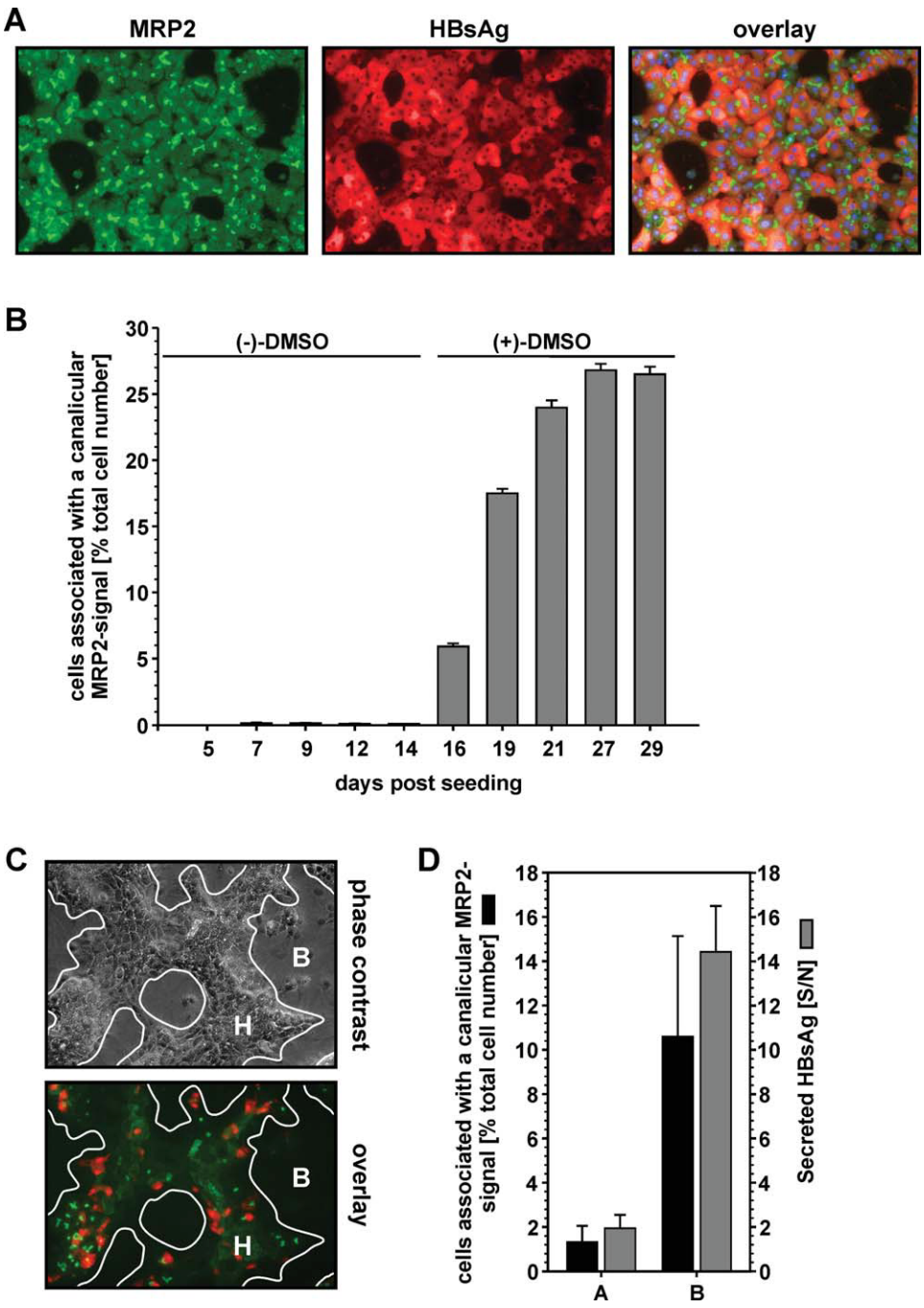

Fig. 3. Polarization and differentiation state of PHH and HepaRG cells and its influence on susceptibility to HBV. (A) PHHs were infected with 8×10^4 HBV ge/cell. MRP2- and HBsAg-specific IF was performed on day 12 p.i. Depicted is a MRP2-specific IF (green), an HBsAg-specific IF (red), and an overlay of the IF pictures with the nuclei stain (blue) at 200× magnification. (B) HepaRG cells were seeded on coverslips in 12-well plates. On days 5, 7, 9, 12, 14, 16, 19, 21, 27, and 29 postseeding, an MRP2-specific IF was performed. The number of cells associated with a canalicular MRP2 signal was quantified and presented as a percentage of the total cell number (n = 59,961). (C) Phase-contrast image and overlay of an MRP2- (green) and HBcAg-specific IF (red) of an HBV infection of HepaRG cells at day 12 p.i. (200× magnification; H = hepatocyte-like cells, B = biliary-like cells). (D) Two batches of HepaRG cells, designated A and B, were infected in parallel with HBV. On day 12 p.i., an IF for MRP2 was performed. The number of cells associated with a canalicular MRP2 signal was quantified and presented as a percentage of the total cell number (n = 9,311, black bars). HBsAg secreted from day 8-12 p.i. was determined by ELISA and is given as the S/N ratio (gray bars).

compared to the control (Fig. 4A). These findings were substantiated when the differentiation medium was replaced by Ca^{2+}-free buffer. Preincubation of HepaRG cells for 30 minutes with Ca^{2+}-free buffer in the absence of EGTA led to a 2.3-fold increased infection. Preincubation with both Ca^{2+}-free buffer and EGTA resulted in even higher infection rates (4.3-fold). To exclude postentry effects of EGTA, treatment was performed 24 and 72 hours after initiation of infection (Fig. 4B). No increase in infection efficiency was observed when EGTA was added postinfection, whereas preincubation of the cells with EGTA led to a 1.9- to 2.3-fold increase. Because the efficacy of infection of HepaRG cells varies significantly with the passage number and the individual differentiation and polarization process, we compared the influence of the EGTA-induced enhancement of infection in two cell batches (Fig. 4C). We, therefore, correlated the increase of infection by EGTA with the efficacy of the corresponding infection performed in the absence of the chelator. We found the most profound effect of EGTA in those cells that displayed a relatively weak

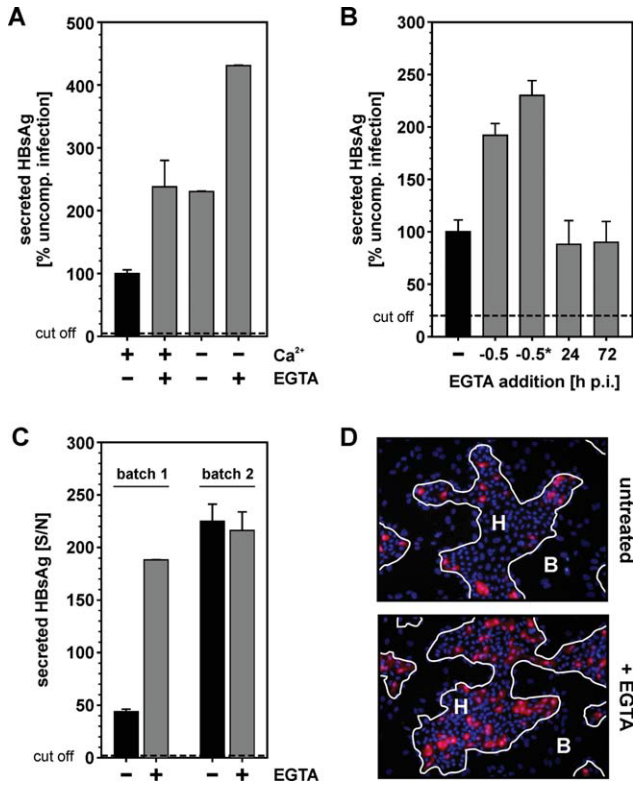

Fig. 4. Temporary disruption of cellular junctions by EGTA and Ca^{2+} depletion. HepaRG cells were incubated with 800 μM of EGTA (30 minutes, 37°C) before infection. Controls without EGTA were performed in parallel. (A) HepaRG cells were pretreated with EGTA in differentiation medium or Ca^{2+}-free buffer and subsequently infected with 8×10^4 HBV ge/cell in the absence of EGTA in differentiation medium. Secreted HBsAg (days 7-11 p.i.) was determined by ELISA. The HBsAg value of the untreated control infection (S/N = 43.68) in differentiation medium was set to 100%. The cut-off of the ELISA is indicated. (B) HepaRG cells were incubated for 30 minutes at 37°C in the presence or absence of EGTA. Preincubation with EGTA was done in Ca^{2+}-free buffer. Inoculation of HepaRG cells with 4×10^4 HBV ge/cell was performed in the absence or presence (*) of EGTA for 24 hours in differentiation medium. Cells were washed and replenished with new medium. Directly (= 24 hours p.i.) or 48 hours (= 72 hours p.i.) after the end of virus inoculation, cells were incubated for 30 minutes at 37°C with EGTA in Ca^{2+}-free buffer. Secreted HBsAg from days 7-11 p.i. was determined by ELISA and is presented as a percentage of the untreated control. (C) HBV infections were performed with two different HepaRG cell batches (1 and 2) after preincubation with EGTA in Ca^{2+}-free buffer. Secreted HBsAg (days 7-11 p.i.) of untreated and EGTA-treated samples were measured by ELISA and are given as S/N. (D) HepaRG cells were preincubated with EGTA in Ca^{2+}-free buffer and infected with HBV in the absence of the chelator. Eight days p.i., an HBcAg-specific IF was performed. For the untreated control and the EGTA-treated sample, an overlay of the nuclear stain (blue) with the HBcAg-specific IF (red) is shown (200× magnification, H = hepatocyte-like cells; B = biliary-like cells).

susceptibility without treatment (4.3-fold induction) (Fig. 4C, batch 1). In contrast, cells that show high amounts of secreted HBsAg already in absence of EGTA could not be further sensitized by Ca^{2+}-removal (Fig. 4C, batch 2). To prove whether enhanced HBsAg-secretion correlates with a higher number of infected cells, and not with enhanced antigen expression per cell, we complemented the HBsAg measurement with HBcAg-specific IF (Fig. 4D). Infection without previous EGTA treatment resulted in the typical staining of single cells, predominantly at the edges of hepatic islands. However, EGTA treatment led to a significant increase in the number of infected cells (1.7-fold). Furthermore, we observed a marked increase of infected cells in the center of hepatic islands. This indicates that the resistant hepatic cells in the center of an island are principally susceptible to HBV infection, but are physically restricted in their accessibility for the virus by tight junctions.

To analyze this in more detail on the single-cell level, we stained HepaRG cells for HBcAg and MRP2 after EGTA treatment and subsequent HBV infection (Fig. 5A). An infection without EGTA was performed in parallel. Quantification of the microscopic analysis revealed no significant differences between the ratios of hepatocyte- to biliary-like cells for the EGTA-treated and control samples (data not shown). In both cases, approximately 67%-70% of cells exhibited a hepatocyte-like morphology. Both cultures showed a similar number of hepatic cells associated with a canalicular MRP2 signal (15%; data not shown). These observations exclude differences in the number of differentiated and polarized hepatic cells as a cause of disparities in HBV infection rates. The majority of HBcAg-positive cells in the untreated sample were located at the edges of hepatic islands (93%; Fig. 5B, left). Infected cells within the islands were associated with canalicular structures. In contrast, pretreatment of HepaRG cells with 800 μM of EGTA led to a 1.3-fold increased number of HBcAg-positive cells and to a change in the distribution of infected cells. Fifty-six percent of infected cells located at the edges of hepatic islands and 44% located inside. Correlation of HBV infection to the polarization of HepaRG cells by means of MRP2 showed that in the untreated control, 82% of infections occurred in cells associated with a canalicular MRP2 signal (Fig. 5B, right). In the EGTA-treated sample, this fraction was reduced to 61%. Simultaneously, the percentage of HBcAg-positive cells not associated with a canalicular MRP2 signal was increased by a factor of 2.2, from 18% to 39%, upon EGTA treatment. These results demonstrate that PHH-like polarization is a prerequisite for infection of HepaRG cells in internal parts of a differentiated island. In contrast, internally located differentiated HepaRG cells not forming canalicular structures are, in principle, susceptible to infection, but restricted by physical barriers.

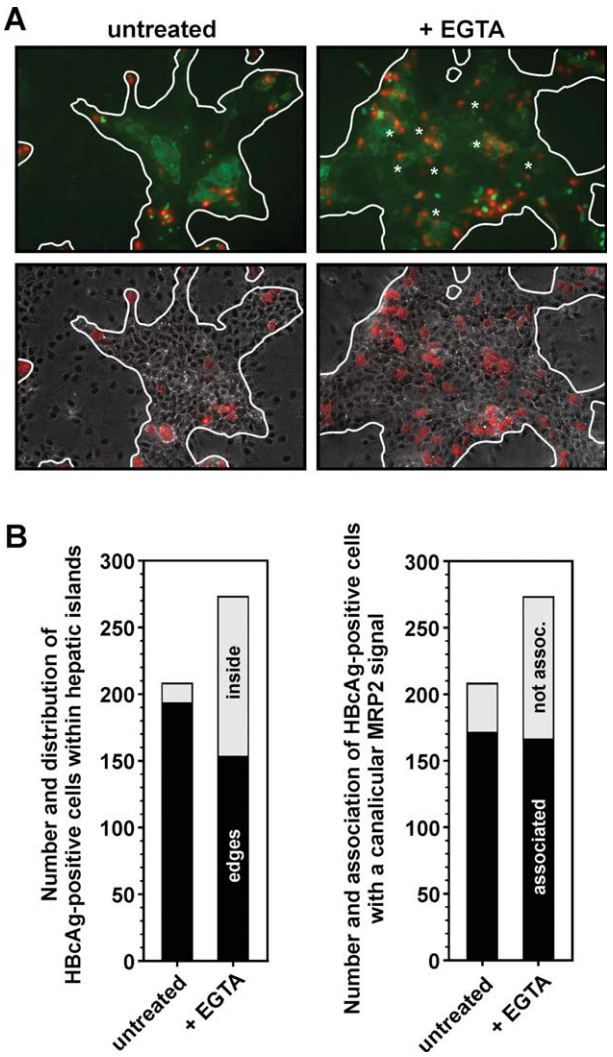

Fig. 5. Susceptibility to HBV of hepatocyte-like HepaRG cells not forming canalicular structures. HepaRG cells were preincubated for 30 minutes at 37°C in the presence or absence of EGTA (800 μM) and infected with HBV in the absence of the chelator. Preincubation with EGTA was performed in Ca^{2+}-free buffer. On day 12 p.i., HBcAg (red)- and MRP2 (green)-specific IF was performed. (A) Representative set of overlay images for the untreated control and the EGTA-treated cells is depicted. HBcAg-positive, hepatic cells not associated with a canalicular MRP2 signal within islands are marked with an asterisk. (B) Quantification of the microscopic analysis shown in (A). In total, 5,754 cells were counted for the analysis. Distribution (left) of HBcAg-positive cells within the hepatic islands, as well as their association with a canalicular MRP2 signal (right), is depicted.

Correlation Between the Percentages of Hepatic, Polarized HepaRG Cells in Culture and HBV Infection Efficiency. The previous observations led to the assumption that an increase in percentage of hepatocyte-like polarized cells with a canalicular MRP2 localization results in higher infection rates at a given virus inoculation dose. To support this hypothesis, we selected a HepaRG culture with a high proportion of canaliculus-containing, hepatocyte-like cells by MRP2-specific IF. We infected this culture with 2.4×10^4 HBV ge/cell and performed HBcAg- and MRP2-specific IF on day 11 p.i. (Fig. 6). The ratio of biliary-like (32%) to hepatocyte-like cells (68%) was comparable to other HepaRG cell batches (data not shown). However, in contrast to other HepaRG cell batches, 56% of cells were associated with a canalicular MRP2 signal (quantification not shown). Quantification of HBcAg-specific IF showed that 12% of total cells were infected under the chosen conditions. Correlation with the percentage of hepatocyte-like cells showed that 18% of hepatocyte-like cells were infected with HBV. In comparison with the experiments shown in Fig. 2, in which 1.7% of total cells where infected with an inoculation dose of 2.5×10^4 ge/cell, this represents a 7-fold increase in infection rates. These observations demonstrate that an increase in percentage of PHH-like polarized cells leads to higher infection rates and thereby also builds the basis for the optimization of the HepaRG infection system.

Discussion

The hepatocytes in the liver are the primary site of HBV replication. They are responsible for liver functions, such as bile production, detoxification, or protein synthesis. To be functional, hepatocytes must be differentiated and polarized. The human hepatoma cell line, HepaRG, has an ability to differentiate toward hepatocyte- and biliary-like cells. This offered us the unique possibility to study and compare the contribution of differentiation and hepatocyte polarization on HBV infection in HepaRG cells and PHHs.

In vivo, studies in chimpanzees showed that 10^1 HBV ge are sufficient to infect and allow virus spread to 100% of hepatocytes.[23] Using cultures of PHHs, we showed that infection rates of up to 100% are also possible *in vitro* (Fig. 1A,B). However, this requires inoculation of the cells with $\geq 0.8 \times 10^4$ ge/cell. Despite the high mge, infection can be blocked with a myristoylated HBVpreS1-peptide, indicating that this infection occurs via the authentic pathway. Similarly to PHHs, HBV infection of HepaRG cells is dependent on the concentration of the virus inoculum and the time of virus inoculation (Fig. 2C,D). In contrast to PHHs, mge up to 40×10^4 led to the infection of only 7% of HepaRG cells. This restriction is not the result of a limitation of infectious virions in the inoculum, because a second round of infection, using the supernatant of the initial infection, led to comparable numbers of infected cells (Fig. 2B). Hantz et al. previously showed that regardless of the virus amount used (up to an mge of 200), a maximum of 20% of cells

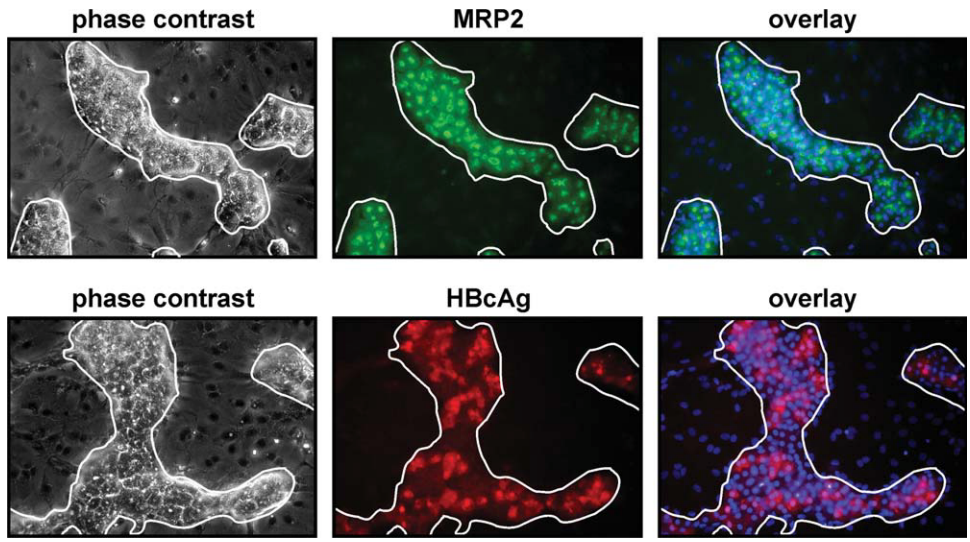

Fig. 6. Effect of the increase in the number of hepatic HepaRG cells associated with a canalicular MRP2 signal on HBV infection efficacy. HepaRG cells were infected with 2.4×10^4 HBV ge/cell. At day 11 p.i., HBcAg- and MRP2-specific IF was performed. A representative set of pictures containing the phase-contrast image, the corresponding IF (MRP2, upper row or HBcAg, lower row) and the overlay of the IF with the nuclear stain (blue) is shown (200× magnification).

(= 40% of hepatocyte-like cells expressing albumin) could be infected.[24]

The slow kinetics and concentration dependency of HBV infection of HepaRG cells argue for an initial, diffusion-controlled mechanism of infection with an unusually low percentage of productive cell association of the virus within a given time. Beyond that, the limitation of infection to only a subset of hepatic cells predominantly located at the periphery of islands (Fig. 2A), as well as the increase of infection after transient disruption of calcium-dependent cell-cell junctions by EGTA, indicates a physical restriction caused by the polarization state of the hepatocyte. HBV thus is similar to other viruses known to depend on the polarization state of cells for successful virus entry.[25,26]

Functional expression of sinusoidal and canalicular hepatic drug transporters, including MRP2 in HepaRG cells and PHHs, has been investigated by Le Vee et al. in proliferating (3 days after seeding), confluent (2 weeks after seeding), and DMSO-treated (4 weeks after seeding) cells by reverse-transcriptase quantitative polymerase chain reaction and drug transport assays.[27] Differentiated HepaRG cells display a transporter expression similar to that in PHHs (i.e., they exhibit substantial messenger RNA [mRNA] levels of influx and secretion transporters). Functional activities of the transporters were verified in HepaRG and PHHs by transport assays. mRNA levels observed for MRP2 were comparable between proliferating, confluent, and DMSO-treated HepaRG cells. We complemented these data by analyzing the MRP2 expression pattern at the protein level by IF over the 4-week cultivation and differentiation process (Fig. 3B; Supporting Fig. 1). Even if MRP2 mRNA levels are comparable in proliferating, confluent, and DMSO-treated HepaRG cells,[27] we, here, demonstrate significant differences in the pattern of MRP2 localization. The canalicular MRP2-signal appears two days after the start of DMSO treatment in IF, indicating that DMSO addition leads to the formation of hepatocyte-like polarity. DMSO is known to induce and maintain cell differentiation in several cell systems, including hepatocytes.[28] The exact role of DMSO in the differentiation process, however, remains poorly understood.

HBV infection of HepaRG cells in internal parts of islands of differentiated cells is restricted to cells that exhibit a PHH-like polarization with canalicular structures (Fig. 3C and scheme in Fig. 7C). The canalicular membrane represents the apical part of the cell. In a noncanalicular, differentiated HepaRG cell, the basolateral membrane is at the sides (i.e., lateral) and on the bottom (i.e., basal), whereas the entire surface of the cell is the apical membrane (Fig. 7B). Assuming that the receptor is basolaterally localized, the virus has no access to its receptor(s). However, if cells form canalicular structures, the apical part is restricted to the canaliculus, whereas the basolateral membrane, including the cell surface, allows interaction with the virus. Because PHHs uniformly display this canalicular-associated phenotype, infection of 100% of cells is possible (Fig. 1 and scheme in Fig. 7A). Similarly, the preferred infection of HepaRG cells at the edges of islands of differentiated cells can be explained by an increased accessibility to the lateral side of the cells, which is not excluded by tight junction formation (Fig. 7B,C). Preincubation of HepaRG cells with EGTA opens Ca^{2+}-dependent cell junctions and thereby enables interaction of HBV with the basolateral localized receptor and subsequent infection (Fig. 7D).

The observation that HepaRG cultures containing higher percentages of PHH-like polarized hepatic cells

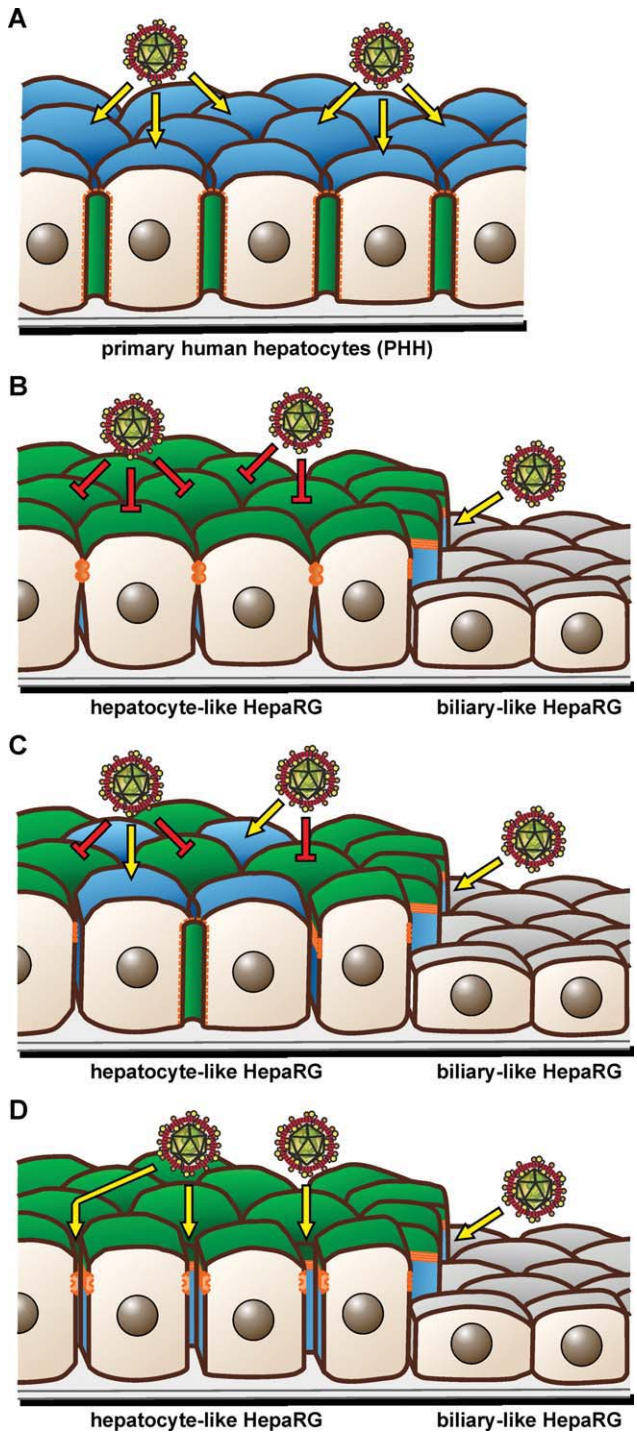

Fig. 7. Model of the role of cell polarization for *in vitro* HBV infection. Schematically depicted is the orientation of the apical (green) and basolateral (blue) membranes of PHH (A) and HepaRG cells (B-D) and the role for HBV infection. For HepaRG cells (B-D), hepatic (left) and biliary-like cells (right) are indicated. Models for hepatic HepaRG cells displaying an epithelial-like phenotype without formation of canaliculi (B) or a mixture of PHH-like (containing canaliculi) and epithelial-like cells (C), as well as HepaRG cells after EGTA treatment (D), are shown. Cell junctions are colored in orange.

display higher infection rates (Fig. 6, in comparison to Fig. 2) builds a basis for the optimization of the infection system. One possible approach for this includes further increasing the percentage of hepatic, PHH-like polarized HepaRG cells by culturing and differentiating them in the presence of combinations of different growth factors and other possible inducers of hepatocyte polarization. Parent et al. already showed that the addition of epidermal growth factor during the cultivation and differentiation of HepaRG cells leads to a differentiation pattern toward hepatocyte-like cells, exhibiting more canalicular structures.[29] To overcome the restrictions of monolayer culture of HepaRG in two dimensions concerning accessibility to the HBV receptor(s), three-dimensional cultures (e.g., in sandwich or as spheroids) would represent an interesting alternative.

However, even in HepaRG cultures having a high percentage of PHH-like polarized cells, not every hepatic cell associated with a canalicular MRP2 signal is infected (Fig. 6). These data indicate that in addition to the physical barrier, other factors (e.g., the antiviral state of the cell and immune responses) restrict HBV infection *in vitro*. In fact, HBV infection of HepaRG cells can be strongly influenced by a previous induction of the interferon response (unpublished data).

In conclusion, our results, at least partially, explain the observed restrictions in the *in vitro* HBV infection system, HepaRG, and simultaneously provide a model for HBV entry, in which HBV infection is, in addition to differentiation, also dependent on the polarization state of the cell (Fig. 7). Formation of hepatocyte-like structures and the resulting transformation in membrane polarity render a HepaRG cell susceptible to infection by allowing access to basolaterally localized HBV-specific receptor(s). Our data, strongly arguing for a polarized entry of HBV via the basolateral domain of the cells, are in agreement with the *in vivo* situation, in which the virus enters the liver through the blood and, initially, has access to the basolateral sides of the hepatocytes facing the sinusoids. Future investigations will analyze, in more detail, the interaction of the virus with possible receptors on the basolateral domain of the hepatocytes and address the question of whether also virus egress occurs in a polarized way.

Acknowledgment: The authors are grateful to Stephanie Held and Martina Spille for their excellent technical assistance and Heinz Schaller, Dietrich Keppler, and Daniel Rost for their provision of antibodies. The authors also thank Stefan Mehrle for his excellent discussions and support. The authors are indebted to Ralf Bartenschlager, who continuously supports our work. The authors thank the Deutsche

Forschungsgemeinschaft FOR1202 "Mechanisms of persistence of hepatotropic viruses" for their support.

References

1. Seeger C, Mason WS. Hepatitis B virus biology. Microbiol Mol Biol Rev 2000;64:51-68.
2. Glebe D, Urban S. Viral and cellular determinants involved in hepadnaviral entry. World J Gastroenterol 2007;13:22-38.
3. Mason A, Wick M, White H, Perrillo R. Hepatitis B virus replication in diverse cell types during chronic hepatitis B virus infection. HEPATOLOGY 1993;18:781-789.
4. Stoll-Becker S, Repp R, Glebe D, Schaefer S, Kreuder J, Kann M, et al. Transcription of hepatitis B virus in peripheral blood mononuclear cells from persistently infected patients. J Virol 1997;71:5399-5407.
5. Kock J, Theilmann L, Galle P, Schlicht HJ.Hepatitis B virus nucleic acids associated with human peripheral blood mononuclear cells do not originate from replicating virus. HEPATOLOGY 1996;23:405-413.
6. Quasdorff M, Protzer U. Control of hepatitis B virus at the level of transcription. J Viral Hepat 2010;17:527-536.
7. Sells MA, Chen ML, Acs G. Production of hepatitis B virus particles in Hep G2 cells transfected with cloned hepatitis B virus DNA. Proc Natl Acad Sci U S A 1987;84:1005-1009.
8. Ladner SK, Otto MJ, Barker CS, Zaifert K, Wang GH, Guo JT, et al. Inducible expression of human hepatitis B virus (HBV) in stably transfected hepatoblastoma cells: a novel system for screening potential inhibitors of HBV replication. Antimicrob Agents Chemother 1997;41:1715-1720.
9. Gripon P, Diot C, Theze N, Fourel I, Loreal O, Brechot C, et al. Hepatitis B virus infection of adult human hepatocytes cultured in the presence of dimethyl sulfoxide. J Virol 1988;62:4136-4143.
10. Walter E, Keist R, Niederost B, Pult I, Blum HE. Hepatitis B virus infection of tupaia hepatocytes *in vitro* and *in vivo*. HEPATOLOGY 1996;24:1-5.
11. Gripon P, Rumin S, Urban S, Le Seyec J, Glaise D, Cannie I, et al. Infection of a human hepatoma cell line by hepatitis B virus. Proc Natl Acad Sci U S A 2002;99:15655-15660.
12. Blanchet M, Sureau C. Infectivity determinants of the hepatitis B virus pre-S domain are confined to the N-terminal 75 amino acid residues. J Virol 2007;81:5841-5849.
13. Gripon P, Le Seyec J, Rumin S, Guguen-Guillouzo C. Myristylation of the hepatitis B virus large surface protein is essential for viral infectivity. Virology 1995;213:292-299.
14. Jaoude GA, Sureau C. Role of the antigenic loop of the hepatitis B virus envelope proteins in infectivity of hepatitis delta virus. J Virol 2005;79:10460-10466.
15. Le Seyec J, Chouteau P, Cannie I, Guguen-Guillouzo C, Gripon P. Infection process of the hepatitis B virus depends on the presence of a defined sequence in the pre-S1 domain. J Virol 1999;73:2052-2057.
16. Leistner CM, Gruen-Bernhard S, Glebe D. Role of glycosaminoglycans for binding and infection of hepatitis B virus. Cell Microbiol 2008;10:122-133.
17. Schulze A, Gripon P, Urban S. Hepatitis B virus infection initiates with a large surface protein-dependent binding to heparan sulfate proteoglycans. HEPATOLOGY 2007;46:1759-1768.
18. Perrault M, Pecheur EI. The hepatitis C virus and its hepatic environment: a toxic but finely tuned partnership. Biochem J 2009;423:303-314.
19. Cerec V, Glaise D, Garnier D, Morosan S, Turlin B, Drenou B, et al. Transdifferentiation of hepatocyte-like cells from the human hepatoma HepaRG cell line through bipotent progenitor. HEPATOLOGY 2007;45:957-967.
20. Weiss TS, Pahernik S, Scheruebl I, Jauch KW, Thasler WE. Cellular damage to human hepatocytes through repeated application of 5-aminolevulinic acid. J Hepatol 2003;38:476-482.
21. Gripon P, Cannie I, Urban S. Efficient inhibition of hepatitis B virus infection by acylated peptides derived from the large viral surface protein. J Virol 2005;79:1613-1622.
22. Borst P, Elferink RO. Mammalian ABC transporters in health and disease. Annu Rev Biochem 2002;71:537-592.
23. Asabe S, Wieland SF, Chattopadhyay PK, Roederer M, Engle RE, Purcell RH, et al. The size of the viral inoculum contributes to the outcome of hepatitis B virus infection. J Virol 2009;83:9652-9662.
24. Hantz O, Parent R, Durantel D, Gripon P, Guguen-Guillouzo C, Zoulim F. Persistence of the hepatitis B virus covalently closed circular DNA in HepaRG human hepatocyte-like cells. J Gen Virol 2009;90:127-135.
25. Bilello JP, Delaney WE, Boyce FM, Isom HC. Transient disruption of intercellular junctions enables baculovirus entry into nondividing hepatocytes. J Virol 2001;75:9857-9871.
26. Esclatine A, Lemullois M, Servin AL, Quero AM, Geniteau-Legendre M. Human cytomegalovirus infects Caco-2 intestinal epithelial cells basolaterally regardless of the differentiation state. J Virol 2000;74:513-517.
27. Le VM, Jigorel E, Glaise D, Gripon P, Guguen-Guillouzo C, Fardel O. Functional expression of sinusoidal and canalicular hepatic drug transporters in the differentiated human hepatoma HepaRG cell line. Eur J Pharm Sci 2006;28:109-117.
28. Isom HC, Secott T, Georgoff I, Woodworth C, Mummaw J. Maintenance of differentiated rat hepatocytes in primary culture. Proc Natl Acad Sci U S A 1985;82:3252-3256.
29. Parent R, Marion MJ, Furio L, Trepo C, Petit MA. Origin and characterization of a human bipotent liver progenitor cell line. Gastroenterology 2004;126:1147-1156.